

# Blue light potentiates neurogenesis induced by retinoic acid-loaded responsive nanoparticles

**AUTHORS:** Tiago Santos <sup>1</sup>, Raquel Ferreira <sup>1</sup>, Emanuel Quartin<sup>2</sup>, Carlos Boto <sup>2</sup>, Cláudia Saraiva <sup>1</sup>, José Bragança <sup>3</sup>, João Peça <sup>4,5</sup>, Cecília Rodrigues<sup>6</sup>, Lino Ferreira <sup>2,4,5</sup>, Liliana Bernardino <sup>1</sup>

<sup>1</sup>Health Sciences Research Centre (CICS-UBI), University of Beira Interior, 6200-506 Covilhã, Portugal.

<sup>2</sup>Biocant - Center of Innovation in Biotechnology, 3060-197 Cantanhede, Portugal.

<sup>3</sup>Institute for Biotechnology and Bioengineering, Centre for Molecular and Structural Biomedicine (CBME), University of Algarve, 8005-139 Faro, Portugal.

<sup>4</sup>CNC - Center for Neuroscience and Cell Biology, University of Coimbra, 3004-517 Coimbra, Portugal.

<sup>5</sup>Institute for Interdisciplinary Research, University of Coimbra (IIIUC), 3030-789 Coimbra, Portugal.

<sup>6</sup>Research Institute for Medicines (iMed.Ulisboa), Faculty of Pharmacy, University of Lisbon, Lisbon, Portugal.

## **CORRESPONDING AUTHOR:**

Liliana Bernardino: Health Sciences Research Centre (CICS-UBI), University of Beira Interior, Av. Infante D. Henrique, 6200-506 Covilhã

Phone: +351 965361114

Email: [libernardino@fcsaude.ubi.pt](mailto:libernardino@fcsaude.ubi.pt)

## **ABSTRACT**

Neural stem cells are a powerful endogenous source of new neurons with vast potential for brain repair strategies. Neuronal differentiation of these cells can be induced by molecules such as retinoic acid (RA). Importantly, mild levels of reactive oxygen species (ROS) are also capable of inducing neuronal differentiation and upregulating RA receptor alpha (RAR $\alpha$ ). The results show that laser light can be used as a trigger of RA release from light-responsive polymeric nanoparticles and ROS production to enhance the neurogenic potential of RA. Blue light stimulation (405 nm laser) demonstrates neurogenic capabilities by itself through the transient induction of NADPH oxidase-mediated ROS and associated  $\beta$ -catenin activation. Furthermore, light stimulation upregulates RAR $\alpha$ , resulting in enhanced RA-induced neurogenesis both in vitro and in vivo. In conclusion, this combinatory treatment offers great advantages to potentiate neuronal differentiation of neural stem cells, allowing a temporal and spatial control of intracellular RA release, while inducing an amplification of its neurogenic effect.

**KEYWORDS:** light responsive, nanoparticles, neural stem cells, neuronal differentiation, polymeric, retinoic acid.

### **1. Introduction**

The subventricular zone (SVZ), located between the ependymal layer of the lateral ventricles and the parenchyma of the *striatum*, is the largest neurogenic niche in the adult human and mammalian brain [1]. Within this region, self-renewing multipotent neural stem cells (NSCs) have the ability to differentiate into neurons, astrocytes, and oligodendrocytes [2, 3]. The persistence of this germinal region throughout life supports the idea that new cells

may be used to restore dysfunctional or damaged circuitries. Importantly, endogenous SVZ cells have been shown to proliferate, migrate and differentiate in response to brain injury, and ultimately induce functional repair. Indeed, the proliferation rate of SVZ cells is increased after seizures, ischemia, spinal cord transection, among others [4]. The plasticity exhibited by the adult brain after injury [5], suggests that pro-neurogenic factors may be good candidates for enhancing regeneration of the injured brain. In this context, a molecule of particular interest is retinoic acid (RA). RA is a metabolic product of retinol (vitamin A) that regulates cell proliferation, differentiation and apoptosis in the developing and adult mammalian brain [6, 7]. The involvement of RA on adult neurogenesis is well documented. Depletion of RA in adult mice leads to decreased neuronal differentiation and cell survival within the subgranular zone of the hippocampus [8]. Similarly, administration of an inhibitor of RA synthesis (disulfiram) to neonatal mice decreased cell proliferation in the SVZ, and electroporation of dominant-negative RA receptors altered the morphology of neuronal progenitors and blocked neuroblast migration [9]. Importantly, defective RA signalling has been implicated in the onset of brain diseases [10, 11]. In the nucleus, RA signalling is transduced by RA receptor (RAR) and retinoid X receptor (RXR), activating gene transcription. RAR also regulates non-nuclear and non-transcriptional effects, namely the activation of kinase cascades [12]. Of note, it was recently reported that moderate ROS stabilize RAR $\alpha$ , the most abundant RAR isotype [13]. In fact, this study reported that direct exposure to low concentrations of hydrogen peroxide increased RAR $\alpha$  protein levels. With increased RAR $\alpha$  levels, RA responsiveness is expected to increase. In addition to this effect, moderate ROS are also capable of inducing NSC differentiation [14].

In the present work, we propose to assess the contribution of laser light to induce ROS-mediated neurogenesis and RAR $\alpha$  upregulation, and to trigger the release of RA from light-responsive nanoparticles (LR-NP) to magnify neuronal differentiation. The use of

nanocarriers that can be remotely disassembled to release RA with spatial and temporal resolution are of high therapeutic value [15, 16]. Even if LR-NP distribute to other tissues, RA will be released only upon light stimulation, bypassing possible side effects [17]. To maximize the success in triggering RA release from LR-NP, we chose the 405 nm wavelength (blue light) since it belongs to the high energetic region of the visible light spectrum.

Herein, we show that exposure to a 405 nm laser exposure transiently increases ROS production, resulting in neuronal differentiation and increased RAR $\alpha$  levels. Additionally, light stimulation was capable of triggering the release of RA from LR-NP and potentiate its neurogenic potential. This approach offered great advantages regarding temporal and spatial control of RA release and efficiently induced SVZ neurogenesis *in vivo*. The successful development of this platform will provide innovative and efficient applications for brain regenerative therapies by inducing the generation of new neurons from endogenous NSCs which may potentially replace death cells and improve functional recovery.

## 2. Materials and Methods

All experiments were performed in accordance with European Community Council Directives (2010/63/EU) and the Portuguese law (DL n $^{\circ}$  113/2013) for the care and use of laboratory animals.

*2.1. SVZ cell cultures:* SVZ cells were prepared from 1-3 day-old C57BL/6 mice as described previously.<sup>[39]</sup>

*2.2. Preparation of light-responsive RA-loaded nanoparticles:* For the preparation of LR-NP, a solution of RA (24  $\mu$ L, 50 mg mL $^{-1}$ , in DMSO) and a solution of polyethylenimine and 4,5-dimethoxy-2-nitrobenzyl chloroformate (PEI-DMNC) (66.7  $\mu$ L, 150 mg mL $^{-1}$  respectively, in DMSO) were added simultaneously to an aqueous solution of dextran sulphate (DS; 5 mL, 0.4 mg mL $^{-1}$ ) and stirred for 5 min. Then, an aqueous solution of ZnSO $_4$  (120  $\mu$ L, 1 M) was added and stirred for 30 min. The NP suspension was dialyzed (Spectra/Por $^{\circledR}$  1 Regenerated Cellulose dialysis membrane, MWCO 6000-8000 Da,

Spectrum) for 24 h, in the dark, against an aqueous solution of mannitol (5 %, w/v), lyophilized and stored at 4°C before use.

*2.3. RA-release studies:* A solution of [<sup>3</sup>H]RA in DMSO was used for the preparation of LR-NP, using a 1:20 ratio of labeled to unlabeled RA (1nCi μg<sup>-1</sup> RA). The initial RA cargo was quantified using 2/3 of the original LR-NP suspension (1mg ml<sup>-1</sup>). To quantify the controlled release of RA, a 10μg mL<sup>-1</sup> suspension of [<sup>3</sup>H]LR-NP was irradiated with blue light (405 nm). For each timepoint (0s, 30s, 60s, 600s) the NP suspension was centrifuged at 14000g for 3 minutes, the supernatant collected and mixed with liquid scintillation fluid (1 mL; Ultima Gold, Packard Instrument SA, Rungis, France) and the scintillations counted in a TriCarb 2900 TR Scintillation analyser (Perkin Elmer, Buckinghamshire, UK).

*2.4. Cell treatments:* Six-day-old neurospheres were adhered for 2 days onto poly-D-lysine (0.1 mg/mL)-coated 12-well μ-chamber slides (IBIDI, Germany) for all experiments except ROS quantification in which cells were adhered onto poly-D-lysine-coated 96-well plates, all in growth factor (EGF, FGF-2)-devoid medium. SVZ cells were then treated with LR-NP alone, laser alone, or LR-NP for 24 h followed by laser treatment (Z-Laser Optoelektronik GmbH, Freiburg, Germany). Laser aperture was set to cover the area of one well (0.27 cm<sup>2</sup>), with a fixed distance between laser source and cells (5 cm). During laser treatments, cell media was reduced to 80 μL/well to allow better light penetration and reduced dispersion. All the inhibitors used were added to cell media 1 h before treatments, namely apocynin (5 μM, Sigma, St. Louis, MO, USA), a broad NOX inhibitor and IWR-1-endo (5 μM, Santa Cruz Biotechnology, Santa Cruz, CA, USA), a Wnt pathway inhibitor via proteasomal degradation of β-catenin. Controls including Blank LR-NP (void nanoparticles) and DMSO (1:10000) were also performed.

*2.5. PI Incorporation:* PI is a cell death marker incorporated by necrotic and late-apoptotic cells. PI (3 μg mL<sup>-1</sup>, Sigma) was added to cell media 10 min before the end of the 48 h treatments. Cells were fixed using 10% formalin solution, neutral buffered, rinsed with PBS, stained with Hoechst-33342 (2 μg mL<sup>-1</sup>; Life Technologies), and mounted in Dako fluorescent medium (Dakocytomation Inc., Carpinteria, CA, USA). Images of PI uptake

labeling were acquired using a fluorescent microscope (Axioskope 2 Plus; Carl Zeiss, Göttingen, Germany).

*2.6. Intracellular ROS quantification:* SVZ cells plated on 96-well plates were cultured in DMEM/F-12 medium devoid of phenol red and supplemented with 100 U mL<sup>-1</sup> penicillin, 100 µg mL<sup>-1</sup> streptomycin and 1% B27 supplement (all from Life Technologies). Cells were treated with laser alone for different time points and 10 min before the end of the experiment, 2',7'-dichlorodihydrofluorescein diacetate (DCFDA) or MitoSOX red (both from Life Technologies) was added to cell media in order to reach a final concentration of 50 µM and 5 µM respectively. After 10 min, cells were washed with warm medium and emitted fluorescence was read in a microplate spectrophotometer plate reader at Ex/Em(DCFDA): 485/530 nm and Ex/Em(MitoSOX): 510/580 nm.

*2.7. Immunocytochemistry:* Cells were fixed with 10% formalin solution, neutral buffered. After washing three times with PBS, unspecific binding was blocked and cells permeabilized for 30 min, at room temperature (RT) with a solution containing 3% BSA, 0.3% Triton X-100. Cells were kept overnight at 4 °C in primary antibody solution, then washed with PBS and incubated for 1 h at RT with the corresponding secondary antibody. Primary antibodies were used as listed: goat polyclonal anti-sox2 (1:200; Santa Cruz Biotechnology), mouse monoclonal anti-Nestin (1:200; Abcam, Cambridge, UK), mouse monoclonal anti-GFAP (1:200; Cell Signaling Technology, Beverly, MA, USA), goat polyclonal anti-doublecortin (1:100; Santa Cruz), rabbit monoclonal anti-Ki67 (1:100; Abcam), mouse monoclonal anti-NeuN (1:100; Millipore, Spain), mouse monoclonal anti-8-oxo-dG (1:100; Trevigen, Gaithersburg, MD, USA), mouse monoclonal anti-active β-catenin (1:100; Millipore), rabbit polyclonal anti-total β-catenin (1:500; Abcam) all prepared in 0.3% BSA, 0.03% Triton X-100 solution. Secondary antibodies used were as follows: Alexa Fluor 594 donkey anti-mouse, rabbit or goat, Alexa Fluor 488 donkey anti-mouse, rabbit or goat (1:200 in PBS, all from Life Technologies) together with Hoechst 33342 (2 µg ml<sup>-1</sup>; Life Technologies) for nuclear staining. Preparations were mounted in Dako fluorescent medium and images acquired using a confocal microscope (LSM 710; Carl Zeiss).

2.8. *Western Blot*: SVZ cells were washed with 0.15 M phosphate-buffered saline (PBS) and incubated in RIPA lysis buffer [0.15 M NaCl, 50 mM Tris-Base, 1 mM EGTA, 5 mM EDTA, 1% Triton X-100, 0.5% sodium deoxycholate, 0.1% SDS, 10 mM DTT containing a cocktail of proteinase inhibitors (Roche, Basel, Switzerland)] at 4°C. Lysates were collected and protein concentration determined by BCA assay (Thermo Scientific). Samples were boiled for 5 min at 95 °C with Laemmli buffer and stored at -20 °C until use. Proteins (40 µg of total protein) were resolved in 10% SDS polyacrylamide gels at 120V and then transferred to Amersham Hybond PVDF membranes (GE Healthcare, Buckinghamshire, UK) with 0.45 µm pore size in the following conditions: 300 mA, 90 min at 4 °C in a solution containing 10 mM CAPS and 20% methanol, pH 11). Membranes were blocked in Tris-buffer (TBS) containing 0.1% porcine gelatin (Sigma) for 30 min at RT and incubated overnight at 4 °C with goat polyclonal anti-Nox1 (1:250; Santa Cruz), goat polyclonal anti-Nox4 (1:250; Santa Cruz), rabbit polyclonal anti-Rac1(1:250; Santa Cruz), mouse monoclonal anti-active β-catenin (1:1000; Millipore), rabbit polyclonal anti-total β-catenin (1:4000; abcam), rabbit polyclonal anti-RARalpha (1:1000; St. John's Laboratory, London, UK) antibodies, diluted in blocking solution. After rinsing three times with TBS, membranes were incubated for 1 h, at RT, with HRP-conjugated secondary antibody anti-goat, anti-rabbit or anti-mouse (1:5000; all from Santa Cruz) in blocking solution. For endogenous control, mouse monoclonal anti-GAPDH (1:500; Millipore) antibody was used. Protein immunoreactive bands were visualized in a Chemidoc<sup>TM</sup>MP imaging system (BioRad Laboratories, CA, USA), following membrane incubation with NZY supreme ECL reagent (NZYTech, Lisbon, Portugal). Densitometric analysis was performed using ImageJ software (NIH ImageJ; NIH, Bethesda, MD).

2.9. *Co-immunoprecipitation*: Dvl2 co-immunoprecipitation experiments were adapted from elsewhere.<sup>[44]</sup> SVZ cells were treated with laser alone and protein lysates were collected 1 h after in nonyl phenoxyethoxyethanol-40 (NP-40) lysis buffer containing 50 mM Tris pH 7.2, 100 mM NaCl, 0.1% NP-40, 10% glycerol, 1 mM EDTA containing a cocktail of proteinase inhibitors (Roche, Basel, Switzerland) at 4°C. Protein concentration was

determined by BCA assay (Thermo Scientific, Braunschweig, Germany) and 300 µg of total protein from each lysate was pre-cleared using 10 µl of sepharose beads (Preotein A/G PLUS Agarose Immunoprecipitation Reagent, Santa Cruz) during 1 h at 4°C in a microtube rotator. Then, 1/10 of total volume from each sample was stored as input for later processing and remaining volume was split into two equal parts and treated overnight at 4°C with either 1 µg of anti-Dvl2 antibody or 1 µg of IgG normal mouse serum as control (both from Santa Cruz). Antibody-protein complexes were immobilized on 30 µL of sepharose beads for 2 h at 4°C in a microtube shaker. Bound protein was washed thrice with NP-40 lysis buffer before being boiled during 5 min at 95 °C with laemmli buffer. SDS-polyacrylamide gel separation, transfer and signal detection was performed as described in the “Western Blot” section using the following antibodies: mouse monoclonal anti-Dvl2 (1:250), horse radish peroxidase (HRP)-conjugated anti-mouse (1:5000), goat polyclonal anti-NRX (1:250), HRP-conjugated anti-goat (1:5000; all from Santa Cruz).

*2.10. In vivo experiments:* Adult C57BL/6J male mice (8-10 weeks old) were anesthetized with an intraperitoneal injection of ketamine (90 mg/kg of mouse weight; Imalgene 1000, Merial, Lyon, France) and xylazine (10 mg per kg of mouse weight; Rompun 2%, Bayer, Leverkusen, Germany). After reaching full anaesthesia, mice were placed on the stereotaxic frame (Stoelting 51600, Dublin, Ireland). Scalp was disinfected and an incision was made along the midline. With the skull exposed, a Hamilton syringe (Hamilton, Reno, NV, USA) was lowered until the target scales were taken after setting the zero at the bregma point (X, AP: +0.50; Y, ML: +0.9). The skull was drilled and the syringe was lowered until the target (Z, DV: -1.8). The subventricular injection of 0.6 µg/mL LR-NP, void nanoparticles (blank NP) or vehicle (saline) was performed with a Hamilton syringe at a speed of 0.2 µL/min for 10 minutes. Then, the incision was sutured and mice were kept warm during recovery. The following day, animals were anesthetized and a multimode ceramic ferrule-fixed optical fiber (FG105UCA; Thorlabs, Munich, Germany) was stereotaxically placed using the same coordinates used previously. Then, 405 nm laser (driver: CLD1010LP; laser LP405-MF80; Thorlabs) was connected to the ferrule and shone for 60sec at 18J/cm<sup>2</sup> (“60s”

experimental groups) or not (sham: “Fiber” experimental groups). Laser output was previously measured for each fiber-optic implanted using a power meter (meter: PM100D; sensor: S310C; Thorlabs). A solution of BrdU (Sigma; 50 mg per kg of animal weight) dissolved in sterile 0.9% NaCl was administered i.p. in the following three days (every 12 h). Mice were maintained in controlled conditions during the three weeks of experimental procedure before being euthanized.

*2.11. Immunohistochemistry:* Three weeks after laser treatments, mice were deeply anesthetized with a mixture of ketamine and xylazine, and then perfused intracardially with a saline solution followed by 4% PFA. Brains were surgically removed and post-fixed with 4% PFA for 24 h, followed by immersion in a 30% sucrose solution (Fisher Scientific) in PBS until sunk. Thereafter, brains were flash frozen and 40  $\mu\text{m}$ -thick coronal sections of the SVZ were collected in a series of 6 (spaced 240  $\mu\text{m}$  from each other) using a cryostat (CM 3050S, Leica Microsystems, Wetzlar, Germany). Immunostaining of tissue sections was performed as described previously,<sup>[45]</sup> using the following antibodies: rat monoclonal anti-BrdU (1:500, AbD Serotec, Raleigh, NC, U.S.A.), goat polyclonal anti-DCX (1:1000, Santa Cruz Biotechnology, Inc.), Alexa Fluor 488 donkey anti-rat (1:1000, Life Technologies), Alexa Fluor 546 donkey anti-goat (1:1000; Life Technologies) and Hoechst for nuclear staining (1:10000). Photomicrographs were obtained using an AxioObserver LSM 710 confocal microscope (Carl Zeiss).

*2.13 Statistical Analysis:* All experimental conditions were performed in triplicate from 3 independent cell cultures, unless stated otherwise. Immunocytochemistry counting was performed in 5 random fields per replicate from 3 independent cultures. A minimum of 1500 cells were counted *per* culture. Immunohistochemistry counting was performed in 3 equally separated Z-sections of the dorsolateral SVZ for each slice. All counting was performed using ImageJ software. All experiments included untreated controls or treatment with blank nanoparticles whenever LR-NP were used. Data are expressed as mean  $\pm$  standard error of mean (SEM). Statistical significance was determined with GraphPad Prism 5 (Graph pad, San

Diego, CA, USA) by using ANOVA followed by Bonferroni's test or unpaired two-tailed Student's t test, with  $P < 0.05$  considered to represent statistical significance.

### 3. Results

#### 3.1. Light induces neuronal differentiation, RAR $\alpha$ upregulation and mROS production

We aim to use laser light to induce ROS-mediated neurogenesis and RAR $\alpha$  upregulation, and to trigger the release of RA from light-responsive nanoparticles (LR-NP). To establish proof of concept of the proposed strategy, an energetic light was required. Therefore, we selected a wavelength within the most energetic section of the visible light spectrum (405nm). We performed a single laser treatment with increasing duration and found that 60 sec of laser at 300 mW/cm<sup>2</sup> (Fig. 1; 60s), which corresponds to a fluence of 18 J/cm<sup>2</sup> was the longest exposure time that did not affect cell viability (Appendix A, Fig. S1). Based on these results, laser exposure time up to 60 sec was used to evaluate its neurogenic potential. Accordingly, 60 sec of laser exposure significantly increased the number of NeuN (mature neuronal marker)-positive cells 7 days after one single treatment ( $312.9 \pm 8.3\%$ ;  $P < 0.001$ ; Fig. 1A). We then evaluated if these laser settings were also able to increase RAR $\alpha$  protein levels. Notably, we found increased protein levels of RAR $\alpha$  as detected by Western, 12 h after 60 sec of laser treatment ( $248.3 \pm 62.8\%$ ;  $P < 0.05$ ; Fig. 1B).

High-energy wavelengths can induce mitochondrial DNA (mDNA) damage. mDNA damage leads to mitochondrial dysfunction, resulting in higher levels of superoxide production [18]. Accordingly, we observed a significant increase in mitochondrial superoxide 30 min after 60 sec of laser treatment ( $152.7 \pm 7.1\%$ ;  $P < 0.05$ ), reaching its maximum at 1 h ( $158.9 \pm 7.2\%$ ;  $P < 0.05$ ) and reverting back to basal levels at 7 h (Fig. 1C). Treatment with 30 sec of laser exposure was not capable of inducing neuronal differentiation and accordingly, no significant superoxide alterations were observed. Mitochondrial superoxide rapidly

dismutes into hydrogen peroxide (H<sub>2</sub>O<sub>2</sub>) spontaneously or enzymatically [19]. In opposition to the negatively charged superoxide anion, hydrogen peroxide readily permeates biological membranes, thus escaping mitochondria. For that reason, we also evaluated cytosolic H<sub>2</sub>O<sub>2</sub> levels and found a significant increase, 3 h after 60 sec of laser treatment ( $258.7 \pm 17.8\%$ ;  $P < 0.05$ ) peaking at 7 h ( $288.6 \pm 31.2\%$ ;  $P < 0.01$ ), and revert to basal levels after 36 h (Fig. 1D).

Increased mROS levels induced by 60 sec of laser treatment were accompanied by oxidative DNA lesions, as detected by the 8-oxo-7,8-dihydro-2-deoxyguanosine (8-oxodG) staining. This type of lesion was transiently detected 3 h after 60 sec of laser treatment and reverted to basal levels after 6 h (Fig. 1E). However, 8-oxodG was primarily detected in the cytoplasm rather than the cell nucleus, suggesting that only mitochondrial DNA (mDNA) is affected by laser-induced damage, rather than the nuclear DNA.

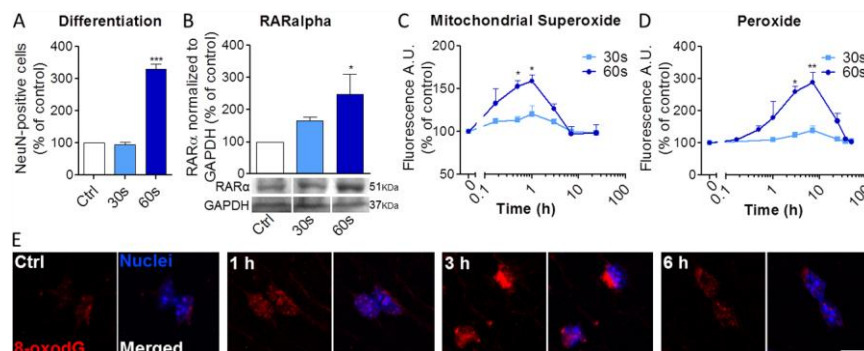


**Figure 1. Laser light stimulation (405 nm) induces differentiation of neural stem cells, upregulates RAR $\alpha$  and transiently induces mitochondrial ROS production.** (A) Graph depicts neuronal differentiation (NeuN-positive cells) 7 days after treatment with 405 nm laser; (B) RAR $\alpha$  protein expression normalized to GAPDH 12 h after treatment; (C) mitochondrial superoxide levels and (D) cytosolic peroxide levels throughout time after 30 or 60 sec of laser exposure (mean  $\pm$  SEM; n=3). \* $P < 0.05$ , \*\* $P < 0.05$ , \*\*\* $P < 0.001$  vs. control using Bonferroni's Multiple Comparison Test. A representative western blot of RAR $\alpha$  (51 kDa) and GAPDH (37 kDa) is shown below the graph in panel B. (E) Representative confocal

digital images of untreated (Ctrl) and 60 sec laser-treated cells labeled for the oxidative damage marker 8-oxo-7,8-dihydro-2-deoxyguanosine (8-oxodG; red), 1 h, 3 h and 6 h after laser treatment. Scale bar = 10  $\mu$ m.

### 3.2. Involvement of the Nox family in ROS generation

Nicotinamide adenine dinucleotide phosphate (NADPH) oxidases (Nox) are superoxide-generating enzymes that participate in several biological processes such as gene expression regulation, and cell differentiation [20]. To evaluate Nox participation in this process, we have selected the time point of highest increase in light-induced cellular ROS (7 h; Fig. 1C and D) to pre-treat cells with apocynin (Apo), a classical Nox inhibitor (Fig. 2A). Apo pre-treated cells presented peroxide levels similar to untreated control and statistically different from 60 sec of laser treatment (Apo+60s:  $101.8 \pm 24.4\%$ ; 60s:  $303.2 \pm 9.8\%$ ;  $P < 0.001$ ), confirming the involvement of Nox enzymes in ROS generation. Then, protein expression of Nox isoforms was assessed by western blot at several time points (1, 3, 6 and 12 h) post treatment. Our results demonstrated that Nox4, the only constitutively active Nox isoform that is also present in mitochondria, is upregulated 1 h after 60 sec of laser exposure ( $263.3 \pm 31.0\%$ ;  $P < 0.05$ ; Fig. 2B). mROS can also trigger Nox1 action by stimulating the Rho GTPase Rac1 [21]. Accordingly, we have detected an increase in both Rac1 ( $167.9 \pm 20.0$ ;  $P < 0.05$ ; Fig. 2C) and Nox1 ( $230.0 \pm 71.1\%$ ;  $P < 0.05$ ; Fig. 2D) expression 3 h after 60 sec of laser treatment.

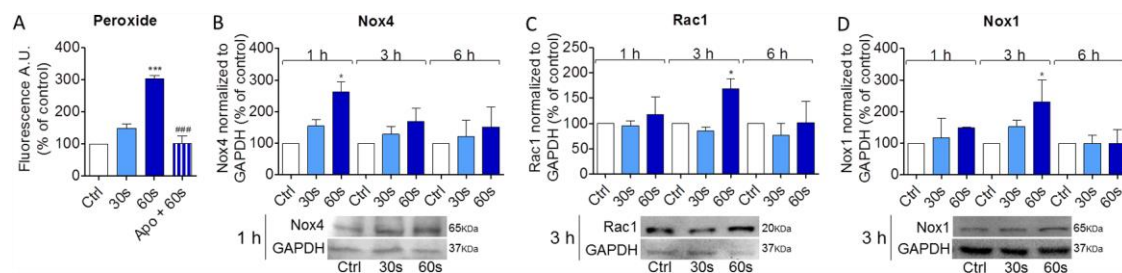


**Figure 2. Laser light treatment (405 nm) increases NADPH oxidase (Nox) and Rac1 expression.** (A) Graph depicts peroxide levels 7 h after treatments; Apo, Apocynin; Data are expressed as percentage of control (mean  $\pm$  SEM; n = 3). \*\*\*P < 0.001 vs control, ###P < 0.001 vs. 60 sec using two-tailed unpaired Student's t-test. Graph depicts the percentage relative to control of (B) Nox4, (C) Rac1 and (D) Nox1 protein expression normalized to GAPDH in cultures exposed to 405 nm laser (30 or 60 sec) after 1, 3, and 6 h. Data are expressed as percentage of control  $\pm$  SEM (n = 3-4). \*P < 0.05 vs control using two-tailed unpaired Student's t-test. Representative Nox4 (65 kDa), Rac1 (20 kDa), Nox1 (65 kDa) and GAPDH (37 kDa) western blots are shown below each graph.

### *3.3. ROS activate $\beta$ -catenin through the dissociation of Dvl2 from NRX*

Hydrogen peroxide is considered the primary type of signaling ROS, acting mainly *via* the oxidation of proteins containing thiol groups [14], such as nucleoredoxin (NRX). In the absence of ROS, NRX interacts with Dishevelled (Dvl), a key player downstream from Wnt receptors, inactivating their functions [22]. However, increased ROS levels oxidize NRX thiol groups leading to structural changes that result in Dvl dissociation. Free Dvl is then capable of activating the Wnt/ $\beta$ -catenin signaling pathway that, among other effects, is known to induce the transcription of neurogenic genes [23]. During the process of NSC neuronal differentiation, Dvl2 was also reported to dissociate from NRX [24]. Accordingly, our co-immunoprecipitation studies confirmed that 60 sec of laser exposure induces the dissociation of the Dvl2:NRX complex 1 h after treatment (Fig. 3A). Again, 30 sec of laser revealed to be insufficient to trigger mechanisms associated with neuronal differentiation. Moreover, this redox sensitive dissociation of Dvl2 was accompanied by an increase in  $\beta$ -catenin activation. Active  $\beta$ -catenin levels were significantly increased as soon as 2 h after 60 sec of laser

treatment ( $196.2 \pm 42.0\%$ ;  $P < 0.05$ ; Fig. 3B, C). Noteworthy, this increase was not detected when cells were pre-incubated with Apo (Nox inhibitor;  $120.5 \pm 15.9\%$ ).

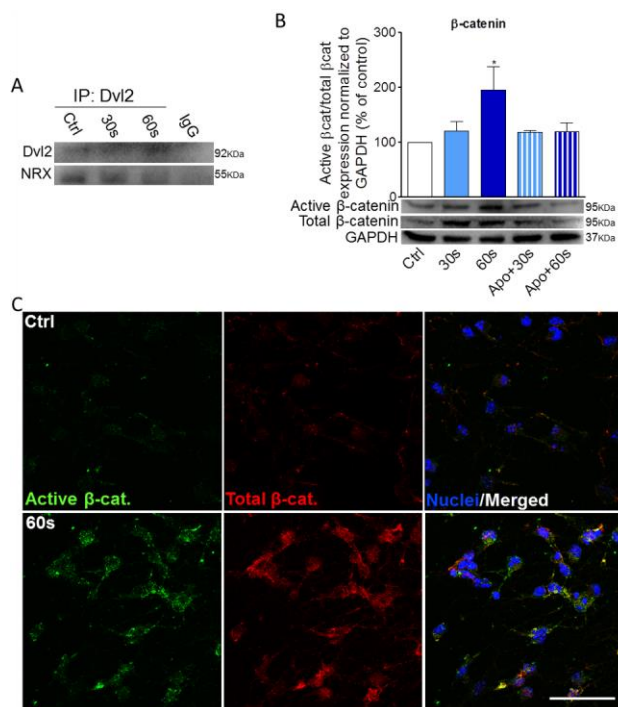


**Figure 3. Laser light (405 nm)-induced ROS activate β-catenin.** (A) Anti-Dvl2 co-immunoprecipitation of neural stem cell lysates 1 h after treatment with 405 nm laser (30 or 60 sec) and mouse IgG co-immunoprecipitation as control; Dvl2 (92 kDa), NRX (55 kDa). (B) Graph depicts the ratio of active β-catenin to total β-catenin levels normalized to GAPDH 2 h after treatment. Apo, Apocynin; Data are expressed as percentage of control (mean ± SEM n=3-4). \* $P < 0.05$  vs. control, using Bonferroni's Multiple Comparison Test. A representative western blot of active β-catenin (95 kDa), total β-catenin (95 kDa) and GAPDH (37 kDa) is shown below the graph. (C) Representative confocal images of active β-catenin (green), total β-catenin (red) and nuclei (blue) in control cultures and in cultures 2 h after laser treatment. Scale bar = 50μm.

### 3.4. Laser light potentiates RA-induced neuronal differentiation of NSCs

To evaluate the effect of RAR $\alpha$  upregulation on RA-induced neuronal differentiation, we pre-treated SVZ cells with RA-containing LR-NP. LR-NP are polymeric nanoparticles composed by poly(ethyleneimine) (PEI), dextran sulfate (DS), 4,5-dimethoxy-2-nitrobenzyl chloroformate (DMNC), a light-responsive photochrome, and RA. Resulting NP present an average diameter of 110 nm, a zeta potential of +25 mV, and a payload of 120 $\mu$ g of RA *per* mg of particle. Before proceeding to cell treatments, LR-NP function was tested by exposing them to blue laser (405 nm, 80 mW) for the duration of 30, 60 and 600 sec, and confirming the presence of RA released by photo-disassembled NP to the aqueous solution (30s:  $4.48 \pm 1.43$ ; 60s:  $3.20 \pm 1.28$ ; 600s:  $22,81 \pm 1.34$  ng of RA/ $\mu$ g of LR-NP; n=3, data not shown)

Regarding LR-NP cytotoxicity, no significant effect on cell death was observed for all the experimental groups tested with NP concentrations up to 20  $\mu$ g/mL, including the conjugation of LR-NP followed by 60 sec of laser exposure (Appendix A, Fig. S2A). The highest non-toxic concentration (20  $\mu$ g/mL) was then selected for cellular internalization studies. DMNC, the photo-cleavable compound used to trigger RA release, has fluorescent properties that enable NP detection by confocal microscopy. Noteworthy, our target population, the multipotent stem/progenitors, internalized LR-NP, namely the Sex determining region Y-box 2 (Sox2)-positive self-renewing and multipotent cells, nestin-positive progenitor cells, glial fibrillary acidic protein (GFAP)-positive cells and doublecortin (DCX)-positive neuronal precursor cells/neuroblasts. (Appendix A, Fig. S2B).

Then, the neurogenic potential of light in combination with RA released from LR-NP was assessed (Fig. 4). Remarkably, the neurogenic effect induced by 60 sec of laser light alone ( $312.9 \pm 8.3\%$ ;  $P < 0.001$ ; Fig. 4A) was further increased when cells were pre-treated for 24 h with 0.6  $\mu$ g/mL LR-NP ( $443.2 \pm 36.4\%$ ;  $P < 0.05$ ) but not when 0.6  $\mu$ g/mL blank NP were used ( $307.2 \pm 9.1\%$ ; data not shown). Interestingly, 30 sec of laser exposure required a higher concentration of LR-NP (2  $\mu$ g/mL) to achieve an amplified neurogenic effect ( $234.8 \pm$

34.5%;  $P < 0.01$ ; Fig. 4A). When repeating the 30 sec laser treatment 24 h after the first stimulation, no differences in neuronal differentiation were detected ( $245.7 \pm 39.2\%$ ;  $P < 0.01$ ; data not shown). For that reason, and to avoid repeated exposure-induced cytotoxicity, we proceeded with one single 405 nm laser treatment protocol. Additionally, LR-NP alone (no laser exposure, 0 sec; Fig. 4A) did not induce a significant increase in neuronal differentiation. Nevertheless, a minor increase in NeuN-positive cells was detected, suggesting that some RA could be leaking from LR-NP.

To confirm the involvement of the previously-mentioned signaling mechanisms, neuronal differentiation was evaluated by NeuN expression in the presence of light alone or in combination with LR-NP, with the addition of Apo (inhibits the initial formation of ROS induced by Nox activation) or IWR-1-endo (IWR; inhibits the later-stage  $\beta$ -catenin action) inhibitors. As predicted, both inhibitors were able to independently suppress neuronal differentiation induced by 60 sec of laser alone (IWR+LR-NP+60s:  $290.8 \pm 19.2\%$ ; Apo+LR-NP+60s:  $194.0 \pm 14.0\%$ ;  $P < 0.05$ ; Fig. 4C). However, for LR-NP+60s, these inhibitors generated different amplitudes of neurogenesis blockage. Altogether, these results indicate that laser-induced ROS and  $RAR\alpha$  levels, in combination with RA released from LR-NP, potentiate the neurogenic response as compared with laser treatment alone.

To better understand the effect of 405 nm laser alone or in combination with LR-NP on the initial steps of cell commitment, Ki67-positive proliferating cells were co-labeled for different neural phenotypes 2 days after treatment. Cell treatments were narrowed to 60 sec of laser stimulation, 0.6  $\mu\text{g/mL}$  of LR-NP or the combination of both. There were no statistically significant alterations detected in the number of total Ki67-positive cells (Fig. 4D) and proliferative Nestin- and Sox2-positive cells (Fig. 4E and F, respectively), suggesting that the stem-like population of self-renewing and multipotent cells was not affected to the detriment of neuronal differentiation. As expected, the number of proliferative DCX-positive

neuroblasts was significantly increased in 60 sec laser ( $65.3 \pm 11.0\%$ ;  $P < 0.05$ ) and LR-NP+60s ( $80.7 \pm 5.1\%$ ;  $P < 0.01$ ) comparing to control ( $40.7 \pm 6.6\%$ ) (Fig. 4G, I). The observed increase in proliferating neuroblasts was accompanied by a decrease in GFAP-positive astrocytic cell proliferation (Fig. 4H, J).

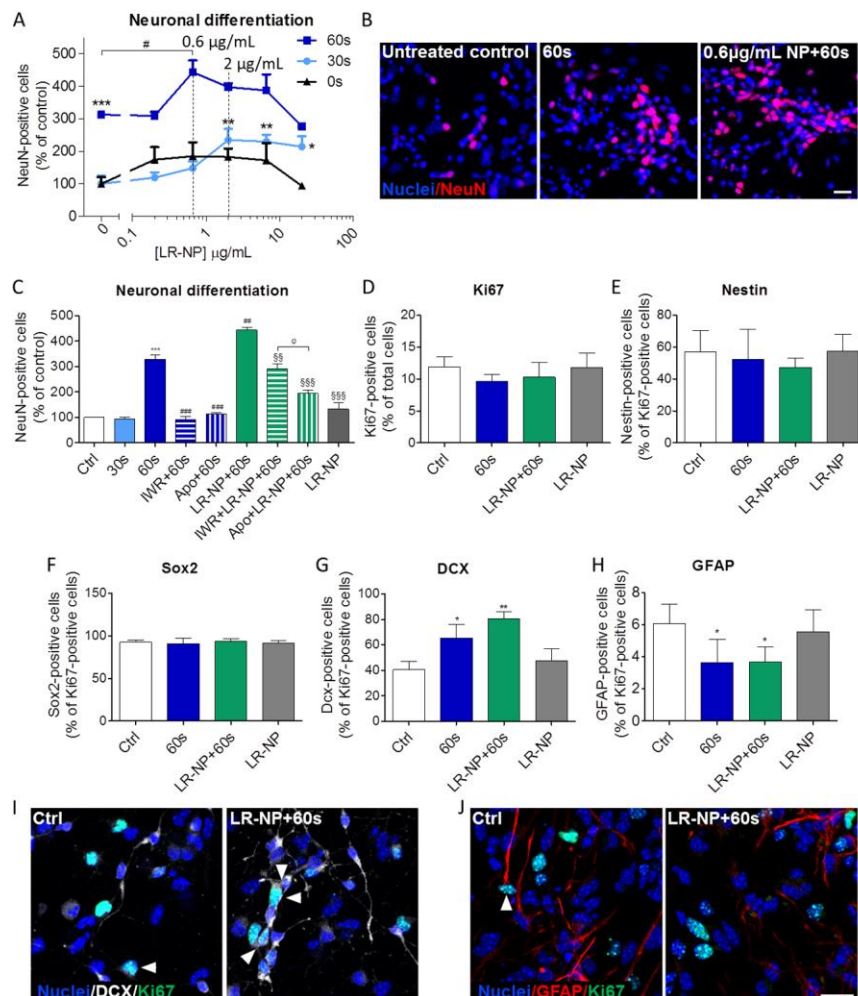


**Figure 4. Light-responsive RA-loaded nanoparticle (LR-NP) treatment in combination with 405 nm laser illumination results in enhanced neuronal differentiation.** (A) SVZ cells were treated with LR-NP (0.2-20 $\mu$ g/mL) alone (0s; no laser exposure) or in combination with a single 405 nm laser pulse during 30 or 60 sec. Percentage of NeuN-positive neurons relative to untreated control cells was determined by immunocytochemistry 7 days after treatment (mean  $\pm$  SEM; n = 3). \* $P < 0.05$ , \*\* $P < 0.05$ , \*\*\* $P < 0.001$  vs. control and # $P < 0.05$  vs. 60s alone using Bonferroni's Multiple Comparison Test. (B) Representative confocal

digital images of NeuN (red) immunocytochemistry (nuclei in blue). (C) SVZ cells were treated with LR-NP (0.6  $\mu\text{g}/\text{mL}$ ) and/or 405 nm laser (30 or 60 sec) alone or in combination with apocynin (Apo) or IWR-1-endo (IWR). Percentage of NeuN-positive neurons relative to untreated control cells was determined by immunocytochemistry 7 days after treatment (mean  $\pm$  SEM; n=3-4). \*P < 0.05, \*\*\*P < 0.001 vs. control; ##P < 0.005, ###P < 0.001 vs. 60s alone; §§P < 0.005, §§§P < 0.001 vs. LR-NP+60s using Bonferroni's Multiple Comparison Test.  $\phi$ P < 0.05 using two-tailed unpaired Student's t-test. (D) Percentage of Ki67-positive cells 2 days after treatment with 60 sec of 405 nm laser, 0.6  $\mu\text{g}/\text{mL}$  LR-NP+60s or 0.6  $\mu\text{g}/\text{mL}$  LR-NP (no laser treatment). Within Ki67-positive cells, different phenotypes were co-labeled, namely (E) Nestin, (F) (Sex determining region Y)-box 2 (Sox2), (G) doublecortin (DCX) and (H) glial fibrillary acidic protein (GFAP) (mean  $\pm$  SEM; n = 3). \*P < 0.05, \*\*P < 0.05 vs. control using two-tailed unpaired Student's t-test. Representative confocal digital images of (I) DCX/Ki67 and (J) GFAP/Ki67 immunostainings. White arrowheads depict double-positive cells. Scale bars = 20 $\mu\text{m}$ .

### 3.5. The combination of LR-NP and light treatment potentiates neuronal differentiation *in vivo*

As proof of concept, we aimed at evaluating the neurogenic potential of LR-NP in combination with 405 nm light *in vivo*. For that, a solution of 0.6  $\mu\text{g}/\text{mL}$  of LR-NP, blank NP or saline was injected in the dorsolateral SVZ region of adult mice and, after 24 h, a laser pulse of 60 sec was applied through an optical fiber using the same stereotaxic coordinates and the same fluence used for *in vitro* studies (18 J/cm<sup>2</sup>). The number of proliferating neuroblasts (DCX+/BrdU+) was evaluated throughout the SVZ (Fig. 5A) and, similarly to *in vitro* results, LR-NP+60s induced the greatest increase in neurogenesis (512.0  $\pm$  177.0%; P < 0.05; Fig. 5A, B) compared to animals injected with saline and fiber-optic uncoupled from laser (sham control; Saline+Fiber: 105.9  $\pm$  30.6%). This increase was more expressive at SVZ

slice number 4, which corresponds to the anteroposterior location of the injection (bregma +0.5), highlighting the spatial resolution of our proposed system. Although there was an increasing trend for the Saline+60s and Blank+60s conditions, these results were not significantly different from Saline+Fiber ( $\approx$  2- to 2.5-fold increase; Fig. 7B).

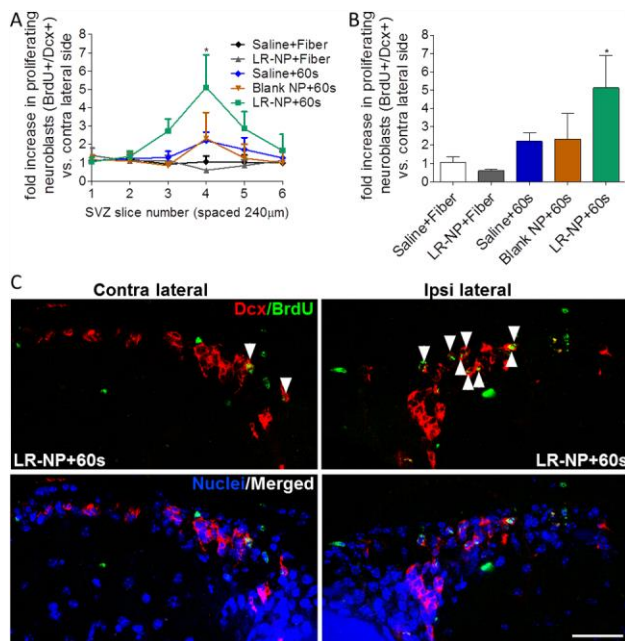


**Figure 5. Enhanced SVZ neuroblast proliferation from light-responsive RA-loaded**

**nanoparticles (LR-NP) together with laser light (405 nm) *in vivo*.** (A) Adult mice were injected with 0.6  $\mu$ g/mL LR-NP, Blank NP or saline and treated on the following day with 405 nm laser during 60 sec or with the laser turned off (sham control: Fiber). Three weeks after treatment, the number of proliferating neuroblasts (DCX+/BrdU+) was counted

throughout the SVZ and normalized to the contra lateral side. (B) Bar graph highlighting the results obtained at the treatment site (SVZ slice number 4) obtained from the previous panel (mean  $\pm$  SEM n=5). \*P < 0.05 vs. Saline+Fiber, using Bonferroni's Multiple Comparison

Test. (C) Representative confocal images of DCX (red), BrdU (green), and nuclei (blue) in contra- and ipsilateral SVZ brain slice number 4 of animals treated with LR-NP+60s. White arrowheads depict double-positive cells. Scale bar = 50 $\mu$ m.

#### 4. Discussion

In our study, we developed a powerful strategy to boost neuronal differentiation by using a 405 nm laser light. Light stimulation transiently increased ROS production, resulting in neuronal differentiation and increased RAR $\alpha$  levels that, in the presence of RA released from LR-NP, enhanced its neurogenic potential.

We first confirmed that the chosen wavelength (405 nm, 300mW/cm<sup>2</sup>) was capable of inducing neuronal differentiation, and increase RAR $\alpha$  levels and ROS production. To the best of our knowledge, there are no reports describing blue light-induced neuronal differentiation of adult NSC. However, blue light-induced differentiation was reported for other stem cell types. As an example, one single exposure to UVB was reported to activate hair follicle melanocyte precursors and originate epidermal melanocytes *via* cell extrinsic mechanisms involving growth factor release [25]. Moreover, a separate study reported that epidermal keratinocytes and epidermal melanocytes secrete Wnt7 upon UVB exposure. Secreted Wnt7 was then responsible for melanocyte stem cell differentiation through the activation of Wnt/ $\beta$ -catenin signaling pathway [26]. Additionally, we have found that mROS were transiently increased upon 60 sec of laser treatment. Physiologically, low levels of mROS work as signaling effectors in processes such as differentiation, autophagy, and metabolic adaptation [14]. Rharass and colleagues demonstrated that the primary trigger for neuronal differentiation upon growth factor depletion in human neural progenitor cells is the generation of mROS. Interestingly, they reported that after growth factor depletion mROS reached a maximum increase of ~200% at 1 h and this increase was significantly but not completely restored at 3 h (no further time points were tested) [24]. Results from Xavier and colleagues are in agreement with our findings, also reporting a transient increase in superoxide mROS 1 h after the induction of NSC differentiation [27]. These results are in line with ours when using 60 sec of laser, indicating that 405 nm laser exposure is capable of triggering processes

similar to those occurring at early stages of NSC differentiation. Additionally, the increase in mROS was accompanied by an increase in cytoplasmic 8-oxodG levels, indicating that mDNA was primarily affected. This is in accordance with the fact that mDNA is more susceptible to lesions during oxidative stress events associated or not with ageing [18].

The laser-induced increase in mROS was Nox dependent, with Nox4, Nox1 and Rac1 upregulated after 60 sec of laser treatment. These enzymes are also implicated in stem cell differentiation. Nox4 was reported to be the only Nox enzyme involved in fate determination and differentiation of neural crest stem cells during embryogenesis [28]. Moreover, Nox4-derived ROS promote embryonic stem cell differentiation into smooth muscle cells [29] or cardiac cells [30]. For cardiovascular differentiation of embryonic stem cells by mechanotransduction, the involvement of both Nox4 and Nox1 enzymes are critical during early stages [31]. Other processes in addition to mROS can also activate the Rac1/Nox1 system during DNA repair. The enzyme 8-oxoguanine DNA glycosylase-1 (OGG1), responsible for 8-oxodG excision, together with free 8-oxodG base pairs released during DNA repair activate Rac1, leading to increased Nox-derived ROS levels [32]. DNA damage also induces phosphorylation of histone H2AX, activating Rac1 GTPase and Nox1, resulting in increased ROS [33]. Importantly, these processes culminate in the activation of Rac1. This enzyme is implicated in neurogenic processes occurring in both adult neurogenic niches, the SVZ and SGZ of the hippocampus. Rac1 is required for normal proliferation, survival and differentiation of SVZ progenitors in the developing forebrain [34], and synaptic plasticity, dendritic spine structure, hippocampal spatial memory and learning-evoked neurogenesis in the SGZ [35, 36].

Notably, our data is in accordance with other processes reported to occur at early stages of ROS-induced NSC differentiation, namely Dvl dissociation and  $\beta$ -catenin activation [24]. Laser-induced neuronal differentiation proved to be ROS and  $\beta$ -catenin dependent, and more

importantly, 405 nm laser upregulated RA receptor RAR $\alpha$ . This clarified the fact that 60 sec of laser induced a greater increase in neuronal differentiation than 30 sec when combined with LR-NP, as the amount of RA released from the nanoparticles is equivalent for both 30 and 60 sec treatment. Importantly, there was a synergistic effect when 0.6  $\mu$ g/mL of LR-NP was combined with 60 sec of laser, compared to laser alone. However, when cells were pre-treated with Apo or IWR, outcomes were different. In particular, IWR+LR-NP+60s-induced differentiation was significantly higher than Apo+LR-NP+60s. By dissecting a proposed mechanism of laser-induced differentiation, we conclude that while Apo inhibits initial ROS formation, IWR inhibits only later-stage  $\beta$ -catenin effects. These results suggest that laser-induced ROS are capable of enhancing RA-induced neuronal differentiation. Importantly, differentiation was less evident when using higher concentrations of LR-NP in combination with laser treatment, indicating that RA-induced neurogenesis is dose dependent. This is in accordance with our previous studies where we reported that RA has an optimal concentration window to drive neuronal commitment of SVZ cells [37]. In contrast to neuronal differentiation results, there was no statistical significance between 60 sec of laser and LR-NP+60s treatments regarding neuroblast proliferation (DCX+/Ki67+). One possibility is that some neural stem/progenitor cells undergo conversion into neurons without cell division. Direct differentiation of stem cells was recently described and is accompanied by a decrease of the NSC pool [38]. Accordingly, there is a decreasing trend for proliferating Nestin-positive cells in LR-NP+60s-treated cells that, if derived from direct conversion, might contribute to the statistical difference at 7 days after treatment. On the other hand, proliferating astrocytes (GFAP+/Ki67+) decreased in a similar fashion when treated with either 60 sec of laser or the combination of LR-NP+60s. We have previously reported that RA-loaded polymeric nanoparticles do not affect NSC astrocytic differentiation [39], as such,

this new result might indicate that decreased astrocytic proliferation is a characteristic restricted to laser-induced differentiation.

To demonstrate the feasibility of this approach, we conducted *in vivo* studies. In accordance with the *in vitro* data, the combination of LR-NP+60s induced the greatest neuronal differentiation *in vivo*. Notably, LR-NP alone did not have any effect, further demonstrating that the nanoparticles are an effective light-responsive delivery agent. Regarding the effect of laser alone, both Saline+60s and Blank+60s induced an increase in proliferating neuroblasts, albeit not statistically significant as compared with saline animals (~2-2.5 -fold increase). Antioxidant coupling between astrocytes and NSCs, such as the induction of glutathione synthesis [40], may eventually reduce intracellular laser-induced ROS levels and its effects, namely on neuronal differentiation, RAR $\alpha$  upregulation and  $\beta$ -catenin activation. Nevertheless, we were able to successfully demonstrate a significant enhancement of the neurogenic potential of RA (released from LR-NP) when combined with laser light *in vivo*. Recent data using low-level laser therapy revealed that near-infrared light (NIR) is capable of improving neurological performance in both patients and animal models of traumatic brain injury [41-43]. Interestingly, 18 J/cm<sup>2</sup> of NIR, the same fluence we used in our study, was able to increase the number of new neurons in the SVZ of mice with traumatic brain injury [43]. Since NIR has high clinical relevance, as it covers the tissue transparency window of the spectrum while sharing similar biological effects with blue light, namely on the induction of neurogenesis and mitochondria-derived ROS, it would be possible to bypass the invasive implantation of fiber-optic required for blue light treatments. For that reason, RA-loaded nanoparticles could be further optimized to include a NIR-responsive molecule to trigger the release of RA.

## 5. Conclusions

We report an innovative and efficient platform to differentiate neural stem cells by using light in combination with light-responsive RA-loaded nanoparticles. We demonstrated the mechanisms by which blue light has neurogenic properties *in vitro*. One single laser pulse of 60 sec ( $300 \text{ mW/cm}^2$ ,  $18 \text{ J/cm}^2$  fluence) transiently induces the generation of mitochondrial Nox-derived ROS to levels similar to those found during earlier stages of neuronal differentiation [24, 27]. Hence, when finely tuned, light is capable of triggering ROS-involved physiological processes such as neuronal differentiation. Other major finding is that light-induced ROS up-regulate the expression of retinoic acid receptor alpha (RAR $\alpha$ ), which enhances RA-induced neurogenesis, highlighting the relevance of our combinatorial treatment for brain regenerative therapies. In fact, based on the capacity to induce mROS, other wavelengths such as NIR, might act *via* similar mechanisms. Additionally, LR-NP can efficiently induce neurogenesis upon laser light (405 nm) exposure by enabling the intracellular delivery of RA, therefore offering great advantages regarding temporal and spatial control of RA release. In this sense, our approach relying on the modulation of SVZ endogenous stem cells for the generation of new neurons is very promising for brain regenerative therapies.

## Disclosure of potential conflicts of interest

The authors declare no conflict of interest.

## Acknowledgements

The authors would like to thank Ana Clara Cristóvão for her contributions. This work was funded by Fundação para a Ciência e Tecnologia (FCT), FEDER and COMPETE; (PTDC/SAU-NEU/104415/2008 , FCOMP-01-0124-FEDER-041099,

SFRH/BD/79526/2011), L'Oréal-UNESCO Portugal for Women in Science, Professor Francisco Pulido Valente Foundation, EC (ERC project no. 307384, "Nanotrigger"), COMPETE (Centro-07-ST24-FEDER-002008), FEDER funds through POCI-COMPETE2020 Operational Programme Competitiveness and Internationalization in Axis-I (Project no. 007491) and by FCT (Project UID/Multi/00709).

## Appendix A. Supplementary data

Supplementary data associated with this article can be found, in the online version.

## References

- [1] Ming G, Song H. Adult Neurogenesis in the Mammalian Brain: Significant Answers and Significant Questions. *Neuron* 2011;70:687-702.
- [2] Gage FH. Neurogenesis in the Adult Brain. *The Journal of Neuroscience* 2002;22:612-3.
- [3] Temple S. The development of neural stem cells. *Nature* 2001;414:112-7
- [4] Picard-Riera N, Nait-Oumesmar B, Baron-Van Evercooren A. Endogenous adult neural stem cells: Limits and potential to repair the injured central nervous system. *J Neurosci Res* 2004;76:223-31.
- [5] Lane MA, Bailey SJ. Role of retinoid signalling in the adult brain. *Prog Neurobiol* 2005;75:275-93.
- [6] Maden M. Retinoid signalling in the development of the central nervous system. *Nature Reviews Neuroscience* 2002;3:843-53.
- [7] Maden M. Retinoic Acid in the Development, Regeneration and Maintenance of the Nervous System. *Nat Rev Neurosci* 2007;8:755-65.
- [8] Jacobs S, Lie DC, DeCicco KL, Shi Y, DeLuca LM, Gage FH, et al. Retinoic acid is required early during adult neurogenesis in the dentate gyrus. *Proceedings of the National Academy of Sciences of the United States of America* 2006;103:3902-7.
- [9] Wang TW, Zhang H, Parent JM. Retinoic Acid Regulates Postnatal Neurogenesis in the Murine Subventricular Zone-Olfactory Bulb Pathway. *Development* 2005;132:2721-32.
- [10] Kawahara K, Suenobu M, Ohtsuka H, Kuniyasu A, Sugimoto Y, Nakagomi M, et al. Cooperative therapeutic action of retinoic acid receptor and retinoid x receptor agonists in a mouse model of Alzheimer's disease. *Journal of Alzheimer's disease : JAD* 2014;42:587-605.
- [11] Anderson DW, Schray RC, Duester G, Schneider JS. Functional significance of aldehyde dehydrogenase ALDH1A1 to the nigrostriatal dopamine system. *Brain Res* 2011;1408:81-7.
- [12] Al Tanoury Z, Piskunov A, Rochette-Egly C. Vitamin A and retinoid signaling: genomic and nongenomic effects: Thematic Review Series: Fat-Soluble Vitamins: Vitamin A. *J Lipid Res* 2013;54:1761-75.
- [13] Cao Y, Wei W, Zhang N, Yu Q, Xu WB, Yu WJ, et al. Oridonin stabilizes retinoic acid receptor alpha through ROS-activated NF-kappaB signaling. *BMC Cancer* 2015;15:248.
- [14] Sena LA, Chandel NS. Physiological roles of mitochondrial reactive oxygen species. *Mol Cell* 2012;48:158-67.

- [15] Fomina N, McFearnin C, Sermsakdi M, Edigin O, Almutairi A. UV and near-IR triggered release from polymeric nanoparticles. *J Am Chem Soc* 2010;132:9540-2.
- [16] Yavlovich A, Smith B, Gupta K, Blumenthal R, Puri A. Light-sensitive lipid-based nanoparticles for drug delivery: design principles and future considerations for biological applications. *Mol Membr Biol* 2010;27:364-81.
- [17] Mura S, Nicolas J, Couvreur P. Stimuli-responsive nanocarriers for drug delivery. *Nat Mater* 2013;12:991-1003.
- [18] Raha S, Robinson BH. Mitochondria, oxygen free radicals, disease and ageing. *Trends Biochem Sci* 2000;25:502-8.
- [19] Finkel T. Signal transduction by reactive oxygen species. *J Cell Biol* 2011;194:7-15.
- [20] Bedard K, Krause KH. The NOX family of ROS-generating NADPH oxidases: physiology and pathophysiology. *Physiol Rev* 2007;87:245-313.
- [21] Lee J, Kotliarova S, Kotliarov Y, Li A, Su Q, Donin NM, et al. Tumor stem cells derived from glioblastomas cultured in bFGF and EGF more closely mirror the phenotype and genotype of primary tumors than do serum-cultured cell lines. *Cancer Cell* 2006;9:391-403.
- [22] Funato Y, Michiue T, Asashima M, Miki H. The thioredoxin-related redox-regulating protein nucleoredoxin inhibits Wnt-beta-catenin signalling through dishevelled. *Nat Cell Biol* 2006;8:501-8.
- [23] Reya T, Clevers H. Wnt signalling in stem cells and cancer. *Nature* 2005;434:843-50.
- [24] Rharass T, Lemcke H, Lantow M, Kuznetsov SA, Weiss DG, Panakova D. Ca<sup>2+</sup>-mediated mitochondrial reactive oxygen species metabolism augments Wnt/beta-catenin pathway activation to facilitate cell differentiation. *J Biol Chem* 2014;289:27937-51.
- [25] Ferguson B, Kunisada T, Aoki H, Handoko HY, Walker GJ. Hair follicle melanocyte precursors are awoken by ultraviolet radiation via a cell extrinsic mechanism. *Photoch Photobio Sci* 2015;14:1179-89.
- [26] Yamada T, Hasegawa S, Inoue Y, Date Y, Yamamoto N, Mizutani H, et al. Wnt/beta-catenin and kit signaling sequentially regulate melanocyte stem cell differentiation in UVB-induced epidermal pigmentation. *The Journal of investigative dermatology* 2013;133:2753-62.
- [27] Xavier JM, Morgado AL, Sola S, Rodrigues CM. Mitochondrial translocation of p53 modulates neuronal fate by preventing differentiation-induced mitochondrial stress. *Antioxid Redox Signal* 2014;21:1009-24.
- [28] Lee JE, Cho KE, Lee KE, Kim J, Bae YS. Nox4-mediated cell signaling regulates differentiation and survival of neural crest stem cells. *Molecules and cells* 2014;37:907-11.
- [29] Xiao Q, Luo Z, Pepe AE, Margariti A, Zeng L, Xu Q. Embryonic stem cell differentiation into smooth muscle cells is mediated by Nox4-produced H<sub>2</sub>O<sub>2</sub>. *Am J Physiol Cell Physiol* 2009;296:C711-23.
- [30] Li J, Stouffs M, Serrander L, Banfi B, Bettiol E, Charnay Y, et al. The NADPH oxidase NOX4 drives cardiac differentiation: Role in regulating cardiac transcription factors and MAP kinase activation. *Molecular biology of the cell* 2006;17:3978-88.
- [31] Sauer H, Ruhe C, Muller JP, Schmelter M, D'Souza R, Wartenberg M. Reactive oxygen species and upregulation of NADPH oxidases in mechanotransduction of embryonic stem cells. *Methods Mol Biol* 2008;477:397-418.
- [32] Hajas G, Bacsı A, Aguilera-Aguirre L, Hegde ML, Tapas KH, Sur S, et al. 8-Oxoguanine DNA glycosylase-1 links DNA repair to cellular signaling via the activation of the small GTPase Rac1. *Free radical biology & medicine* 2013;61:384-94.
- [33] Kang MA, So EY, Simons AL, Spitz DR, Ouchi T. DNA damage induces reactive oxygen species generation through the H2AX-Nox1/Rac1 pathway. *Cell death & disease* 2012;3:e249.

- [34] Leone DP, Srinivasan K, Brakebusch C, McConnell SK. The rho GTPase Rac1 is required for proliferation and survival of progenitors in the developing forebrain. *Developmental neurobiology* 2010;70:659-78.
- [35] Haditsch U, Anderson MP, Freewoman J, Cord B, Babu H, Brakebusch C, et al. Neuronal Rac1 is required for learning-evoked neurogenesis. *J Neurosci* 2013;33:12229-41.
- [36] Haditsch U, Leone DP, Farinelli M, Chrostek-Grashoff A, Brakebusch C, Mansuy IM, et al. A central role for the small GTPase Rac1 in hippocampal plasticity and spatial learning and memory. *Mol Cell Neurosci* 2009;41:409-19.
- [37] Maia J, Santos T, Aday S, Agasse F, Cortes L, Malva JO, et al. Controlling the Neuronal Differentiation of Stem Cells by the Intracellular Delivery of Retinoic Acid-Loaded Nanoparticles. *ACS nano* 2011;5:97-106.
- [38] Barbosa JS, Sanchez-Gonzalez R, Di Giaimo R, Baumgart EV, Theis FJ, Gotz M, et al. Neurodevelopment. Live imaging of adult neural stem cell behavior in the intact and injured zebrafish brain. *Science* 2015;348:789-93.
- [39] Santos T, Ferreira R, Maia J, Agasse F, Xapelli S, Cortes L, et al. Polymeric Nanoparticles to Control the Differentiation of Neural Stem Cells in the Subventricular Zone of the Brain. *ACS nano* 2012;6:10463-74.
- [40] Fernandez-Fernandez S, Almeida A, Bolaños Juan P. Antioxidant and bioenergetic coupling between neurons and astrocytes. *Biochem J* 2012;443:3-11.
- [41] Huang YY, Gupta A, Vecchio D, de Arce VJ, Huang SF, Xuan W, et al. Transcranial low level laser (light) therapy for traumatic brain injury. *Journal of biophotonics* 2012;5:827-37.
- [42] Xuan W, Vatansever F, Huang L, Wu Q, Xuan Y, Dai T, et al. Transcranial low-level laser therapy improves neurological performance in traumatic brain injury in mice: effect of treatment repetition regimen. *PloS one* 2013;8:e53454.
- [43] Xuan W, Vatansever F, Huang L, Hamblin MR. Transcranial low-level laser therapy enhances learning, memory, and neuroprogenitor cells after traumatic brain injury in mice. *Journal of biomedical optics* 2014;19:108003.